

Resin Transfer Molding (RTM) Process of a High Performance Epoxy Resin. II: Effects of Process Variables on the Physical, Static and Dynamic Mechanical Behavior

CHANG-LUN LEE and KUNG-HWA WEI*

*Institute of Materials Science and Engineering
National Chiao Tung University
Hsinchu, 30049, Taiwan, R.O.C.*

The effects of processing variables on the mechanical behavior and the void content of one-part epoxy based glass fabric composites produced by resin transfer molding (RTM) were investigated. The variables studied included injection pressure, injection temperature, and fabric structure. Image analysis was used to measure the void content in the composites. Variations in injection pressure and temperature were found to have a significant effect on the quality and the mechanical performance of composites. The optimized physical and mechanical performance of the composites was obtained by processing the resin at 160°C under 392 kPa pressure. Molding of highly permeable EF420 fabric required a shorter mold filling time, but resulted in reduced flexural strength and storage modulus in the resulting composites as compared with that of the composites containing 1581 fabric.

INTRODUCTION

Fiber reinforced polymer composites have been used extensively as structural components in the aerospace industry and in commercial applications because of their unique directional properties and weight saving potential (1-3). Resin transfer molding (RTM) is a versatile process for manufacturing light-weight and high strength fiber reinforced composite parts. In a typical RTM process, low viscosity reactive resins are injected under pressure into a closed mold cavity filled with a preplaced fiber preform and then are cured at high temperatures to produce fiber reinforced polymeric composites (4-6). Owing to the continuous fiber reinforcement and the low viscosity resin used in the processing, resin transfer molding has been proven to be a cost-effective process for producing high performance composites of complicated geometry and of high strength to weight ratios (7-9).

A microscopic view of resin flow in the RTM process can be described as resin flow through a porous medium during processing. Parnas *et al.* (10) and Chan *et al.* (11, 12) simulated the resin flowing through the macropore and the micropore of the fiber bed simultaneously in the filling stage of RTM. The

macropore is produced around fiber bundles, and the micropore is formed among individual fiber filaments within a fiber bundle. The permeabilities and the impregnation rates in these two regions are different. The voids are brought out as a result of the difference in the impregnation rates between the macropore and the micropore. Lundstrom *et al.* (13) studied the influence of process parameters on the void formation in resin transfer molding of vinyl ester resin. They found that the voids were of two different types: long cylindrical bubbles inside the fiber bundles and larger spheroidal bubbles in the space between the fiber bundles. However, the effect of process parameters on the mechanical behavior of the moldings was not discussed. Patel *et al.* (14) studied the influence of processing variables on resin-fiber interface in liquid composite molding of polyurethane (PU) and polyurethane-unsaturated polyester (PU-UPE) based composites. They found that the fabrics were better wetted and bonded at lower injection pressures and at higher molding temperatures, leading to higher-tensile-strength composites. Rudd *et al.* (15) reported that initial resin temperature, mold temperature and injection pressure affected the cycle time of RTM of polyester composites significantly. Hayward *et al.* (16) studied the effect of process variables on the quality of RTM moldings of glass fiber reinforced polyester resin.

*To whom correspondence should be addressed.

In their study, improvements were found in the mechanical properties and the porosity levels of moldings made with vacuum assistance and the quality of the molded parts decreased slightly with increasing injection pressure.

Although the RTM processes are better understood and more accurately characterized in recent years, the problem of the optimization of the part quality, which is critical for load-bearing structure applications, has not been addressed. Little work has been done with respect to the effect of RTM process variables on part performance for high performance fiber composites, which requires high fiber volume fraction, low void content and the use of a high performance resin system.

The goal of this study is to investigate the effect of RTM processing variables on part performance based on one-part epoxy resin, PR500. Specifically, the injection pressure, resin injection temperature and fabric structures are used as the variables for the RTM processing of PR500 epoxy. The physical, static and dynamic mechanical behavior of the composites produced under different process conditions will be reported.

EXPERIMENTAL

Materials

The epoxy resin PR500, from 3M, is a one-part epoxy. The details of the properties of the resin can be found elsewhere (17). An epoxy-amine resin, LY564/HY2954 from Ciba-Geigy, was used in flow visualization experiments, which exhibits an injectable

viscosity at room temperature. The fabric reinforcements used in this study were a highly permeable glass fabric from Brochier, Injectex EF420-E01-100, with a surface density of 420g/m², and an eight-harness satin woven glass fabric 1581 from Clark-Schwebel Co. with a surface density of 293.3g/m².

Resin Transfer Molding Process

A 32.5 cm by 32.5 cm aluminum flat mold was used in this study. The mold consists of three parts—a bottom plate, a picture frame, and a top plate—as shown in Fig. 1. Rubber gasketing was placed around the perimeter of the mold halves to provide a proper seal. The plates were clamped together with 12 bolts evenly distributed around the edge of the plates. This tool was used to produce 25 cm square flat plate of varying thickness. Placing different size picture frame spacers between the mold halves changed the part thickness. Ten plies of EF420 was used for a 3 mm plate, and ten plies of 1581 was used for a 2 mm plate, producing plates with a fiber volume fraction ~55%. Five holes were machined in the upper mold half, one in the center and the other four in each of the four corners to provide the resin inlet and outlet. The experimental setup of the RTM process is shown in Fig. 2. Initially, the resin was heated to 104°C and was degassed for 30 minutes. The mold containing a fiber preform was heated to 70°C and vacuumed at this temperature for 30 minutes, then heated to 160°C. The resin was injected into the mold under a range of pressures from 293 to 490 kPa. The mold was vented to the atmosphere once the resin injection started. One J-type thermocouple was used for each

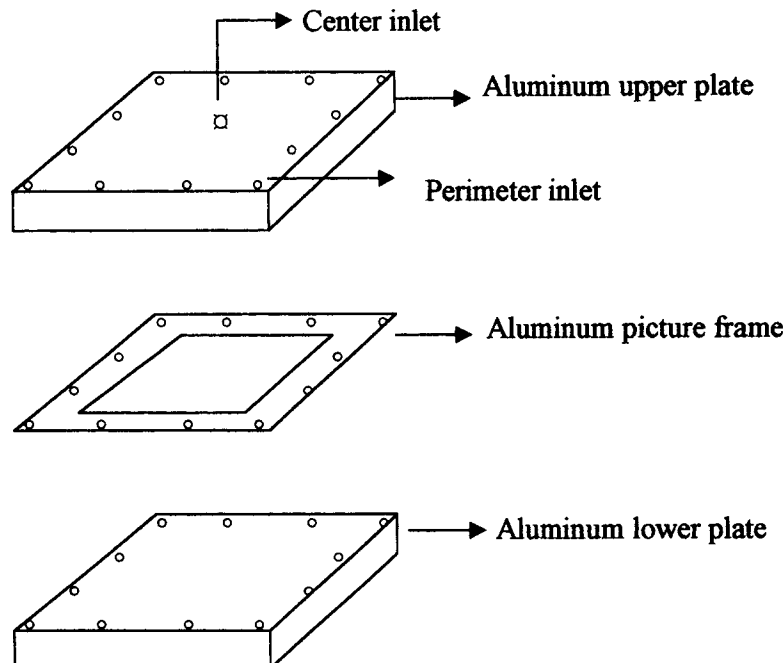


Fig. 1. Schematic diagram of the mold design.

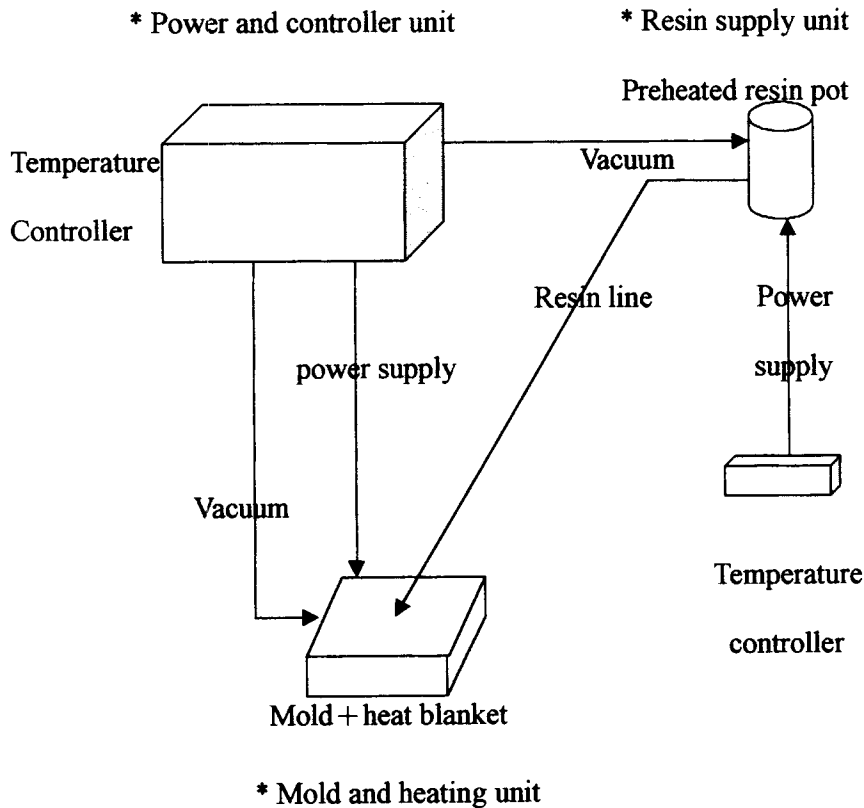


Fig. 2. Schematic diagrams of experimental setup of the RTM process.

case of the center inlet and the perimeter inlet to monitor the temperature throughout the whole process. The location of the thermocouples was near the inlet. There was no pressure transducer used in this study. After the mold was filled, the outlets were opened and closed several times to eliminate any entrapped air in the mold cavity (18). Upon the completion of mold filling, the mold temperature was increased to 177°C for two hours. After cooling, the composite plate was taken out of the mold. The average thickness variation from the center to the edge of the molded samples was 0.18 mm, which indicates that the injection pressure exerted on the mold caused the mold to slightly open. A flow visualization setup was built for following the flow profiles by using an epoxy resin LY564/HY2954 having low viscosity at room temperature. In the flow visualization setup, a transparent acrylic plate was used as the upper mold half in place of the aluminum plate in order to monitor the flow profiles and edge effects during filling stage. The settings of process variables used in this RTM study are given in Table 1.

Process Variables

In this study, a range of pressures from 294 kPa to 490 kPa was used, representing a compromise between flow rate and fiber deformation. The resin injection pressure was changed by adjusting the air pressure in the pressure pot with a Flutterless gauge.

Moldings were performed at injection pressure of 294kPa, 392kPa and 490 kPa. Resin was injected at 160°C and at 150°C for moldings at a center inlet and at a perimeter inlet, respectively. The effect of fabric structure was studied by considering ten layers of 1581 eight-harness satin woven fabric and ten layers of EF420 highly permeable fabric. Each fabric provided around 55% fiber volume fraction for the composites.

Measurements of Viscosity and Dynamic Mechanical Properties

The viscosity-time characteristics of the PR500 neat resin and the dynamic mechanical behavior of the composite specimens were measured using a Rheometrics

Table 1. Settings of Process Variables for PR500 Epoxy Resin.

Variables	Settings
Injection pressure	293–490 kPa
Resin injection temperature	150, 160°C
Resin preheated temperature	104°C
Cure condition	177°C, 2 hrs
Fabric temperature	160°C
Resin viscosity @160°C	250–500 mPa · s
Pack pressure	490 kPa
Fiber volume fraction	55 ± 2%
Thickness of panels	2mm, 3mm

Mechanical Spectrometer, Model RMS-605, following the specification of ASTM D 4473 and ASTM D 4065, respectively. Viscosity measurements were performed with disposable parallel plates of 25 mm diameter subjected to forced oscillations with a gap of 0.5 mm. A time sweep was conducted to obtain the viscosity-time profile at 150°C, and a frequency sweep ranging from 0.1 to 100 Rad/sec on the samples was conducted at 160°C to measure the viscosity of PR500 resin. Samples for the dynamic mechanical test were subjected to rectangular forced torsion at a rate of 6.28 Rad/sec and 0.1% strain over a temperature range of 25 to 250°C. Two specimens were used for each viscosity and each dynamic mechanical measurement. Dynamic mechanical properties including storage modulus (G'), loss modulus (G'') and loss tangent ($\tan \delta$) were measured. The glass transition temperatures of the composites were hereby defined as the temperature under which the $\tan \delta$ reached its maximum value.

Mechanical Properties and Void Content Measurements on Composites

The flexural properties of the composites were measured by three-point bending tests, according to ASTM D 790-92. The selected support span-to-depth ratio was $L:d = 32:1$. The interlaminar shear strength (ILSS) was determined using a short-beam bending rig, according to ASTM D 2344-84. The specimen support span to thickness ratio was 4. Seven specimens were used for each flexural and ILSS tests.

Ultrasonic testing is the most commonly used, and has been proven to be one of the most successful, nondestructive evaluation technique for detecting voids in polymer composites. The RTM plates were inspected by ultrasonic C-scan to evaluate the quality throughout the plates. Samples for void measurement were taken from three different areas of each plate based on ultrasonic C-scan results. The quality of the plates was characterized by the attenuation of the signal. The ultrasonic C-scan of these composites was performed by immersing the plates in water and positioning the plates between two focused 5.0 MHz transducers, one sending and the other receiving. The ultrasonic scan shows variations in ultrasonic attenuation due to such factors as voids, dry spots, resin-rich areas, etc. The smallest detectable void size of ultrasonic detection is set at 0.635 mm. Three threshold levels of the received signal were selected at different

ranges and were presented by color codes in C-scan results. Samples for void measurement were taken from three different areas of each plate based on the color codes in C-scan results. Attenuations of 0%, 25% and 50% are represented by white, orange, and green, respectively. Each void value was obtained by taking average values of three samples. Void content was determined by computerized image analysis. This technique has been used successfully by Hayward and Harris (16) and Ghiorse (19). The samples were mounted in phenolic resin and were finely polished by an automatic Buehler polishing machine. The void content was determined at $\times 40$ magnification, with at least seven random areas chosen from each of the three specimens. The average 21 measurements were calculated and taken to be the volumetric void content of the plate. In this study, the specimen was placed under a Zeiss microscope attached to a RGB vision camera module. The image was fed to a PC based computer with Optimas image analysis software. The software can separate the voids from the background (resin and fibers) via gray level discrimination. The contrast is divided into 256 gray levels. The detection of the samples was carried out with respect to a single threshold. The threshold level and the detection were set such a way that resin and fibers appeared white with respect to the voids.

RESULTS AND DISCUSSION

Effect of Injection Pressure

The interlaminar shear strength (ILSS), flexural strength, flexural modulus and the void content of 1581 fabric composites processed at different injection pressure are given in Table 2. In Table 2, the molding under 392 kPa injection pressure exhibited the optimal physical and mechanical performance with a 6% higher in ILSS, 11% higher in flexural strength and 9% higher in flexural modulus than that of the plates processed at other injection pressures. Moreover, the void content in the plate molded under injection pressure of 392 kPa was at least 30% lower than that of plates molded under other injection pressures. The ILSS value of these plates increased with the decreasing void content. This can be explained by the fact that the high injection pressure of 490 kPa leads to a preferential channeling of the resin through the large pore spaces between fiber tows and reduced the time for the resin to wet the fiber bundles. This resulted in a more erratic flow pattern and non-uniform

Table 2. The Effect of Injection Pressure on the Mechanical Properties of 1581/PR-500 Laminates.

Pressure (kPa)	ILSS (MPa)	Flexural Strength (MPa)	Flexural Modulus (GPa)	Void Content (%)
294	57.2 (4.8)	527.4 (24.8)	29.6 (2.8)	0.37 (0.06)
392	62.0 (2.8)	584.7 (20.7)	32.4 (2.1)	0.19 (0.1)
490	58.6 (4.1)	508.8 (22.8)	29.6 (0.7)	0.26 (0.12)

*Resin transfer with a center inlet.

*Resin injection temperature is 160°C.

() denotes standard deviation.

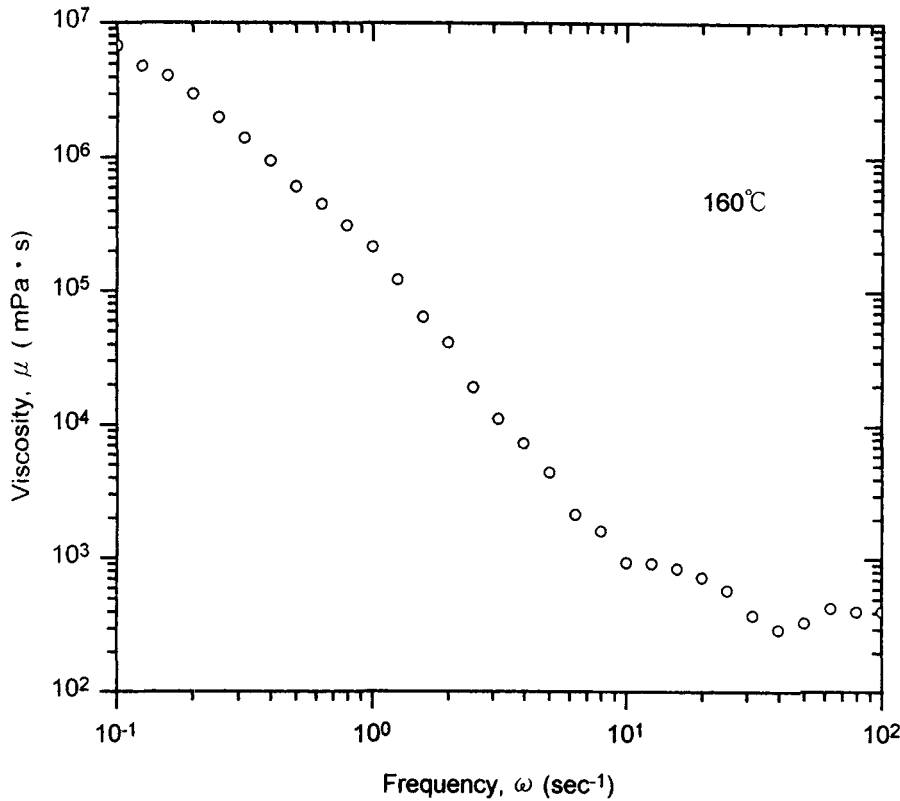


Fig. 3. Frequency/shear rate dependent viscosity of PR500 resin at 160°C.

fronts and therefore caused a high probability of entrapping air bubbles inside the composites (20, 21). A higher void content in these plates was also found in the case of 294 kPa injection pressure as compared with the case of 392 kPa injection pressure. It can be attributed to the high viscosity of the resin because of the shear rate dependent viscosity. The viscosity of PR500 resin decreased in a power law behavior with increasing shear frequency at 160°C, as shown in Fig. 3. The more viscous resin tends to flow around the fiber bundles (macropores) than to flow through the fiber reinforcement (micropores) during the mold filling process. The voids are formed because of the difference of the impregnation rates between the macropores and the micropores (10–12).

The dynamic mechanical properties of these plates exhibited the similar trend as the static mechanical properties of these plates. The plates processed under

392 kPa injection pressure showed the highest storage modulus (G') at $\tan \delta_{max}$ among the three plates, more than 24% higher than the storage modulus of the others, as given in Table 3. It is interesting to note that the storage modulus also decreased with increasing void content. It can be concluded that at the injection pressure of 392 kPa, relatively uniform flow fronts in both the micro- and macro-pores were obtained for PR500 in RTM process. The effect of injection pressure on the mold filling time is given in Table 4. In Table 4, mold filling time decreased with increasing injection pressure as expected.

Table 3. Effect of Injection Pressure on the Dynamic Mechanical Properties of 1581/PR500 Composites.

Pressure (kPa)	T _g (°C)	tan δ	Storage Modulus (G') (MPa)
294	207	0.5064	594.0
392	207	0.4734	963.1
490	208	0.5027	776.2

*Resin transferred with a center inlet.

Table 4. Mold Filling Time as a Function of Injection Pressure.

Pressure (kPa)	Mold Filling Time of Outlet (Sec)			
	#1	#2	#3	#4
294	158	117	145	123
392	78	67	78	105
490	52	56	58	74

*1581/PR-500 System.
 *Resin injection temperature:160°C
 *Outlet #1–4, see right

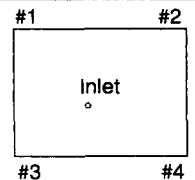


Table 5. Effect of Resin Injection Temperature and Fabric Structure on the Mechanical Behavior and Void Content of PR-500 RTM Composites.

Fabric/Resin	ILSS (MPa)		Flexural Strength (MPa)		Flexural Modulus (GPa)		Void Content (%)	
	160°C	150°C	160°C	150°C	160°C	150°C	160°C	150°C
EF420/PR-500	55.8 (2.1)	66.2 (2.8)	599.8 (15.2)	530.9 (16.5)	26.2 (1.4)	25.5 (0.7)	0.25 (0.05)	0.13 (0.05)
1581/PR-500	62.0 (2.8)	60.7 (2.1)	584.7 (20.7)	543.3 (31.7)	32.4 (2.1)	31.0 (2.8)	0.19 (0.1)	0.19 (0.09)

* 160°C: measured at the center inlet.

* 150°C: measured at the perimeter inlet.

* () denotes standard deviation.

Table 6. Dynamic Mechanical Properties of EF420/PR500 and 1581/PR500 RTM Composites.

Fabric/Resin	Resin Injection Temperature (°C)	T _g (°C)	tan δ	Storage Modulus (G') (MPa)
EF420/PR500	160	185	0.4387	387.2
1581/PR500	150	208	0.4189	386.8
EF420/PR500	160	207	0.4734	963.1
1581/PR500	150	209	0.5234	566.1

Effect of Injection Temperature

For moldings of both EF420 and 1581 fabrics, resin was injected at 160°C for a center inlet, and resin was injected at 150°C for a perimeter inlet. The injection pressure used was 392 kPa. The interlaminar shear strength, the flexural strength and the modulus of these plates are given in Table 5. In Table 5, the differences in the ILSS, the flexural modulus between the plates produced at different temperatures for both fabrics, are small. However, a 7%–11.5% lower flexural strength was found for the plates of both fabrics at 150°C injection temperature as compared with that of the plate at 160°C injection temperature. The void content of the plates containing 1581 fabrics is essentially not affected by the injection temperature, also given in Table 5. The effect of resin injection temperature on the dynamic mechanical properties of these plates is presented in Table 6. In Table 6, there is a 41% reduction in the storage modulus (G') of the 1581/PR500 plate injected at 150°C as compared with that of the 1581/PR500 plate injected at 160°C. There is little change in the storage modulus (G') of EF420/PR500 plate produced at different injection temperatures. A restriction of resin flow was also found in the case of resin injection at 150°C via a perimeter inlet.

The mold filling time of the plates injected at 150°C was larger than that of the plate injected at 160°C, as given in Table 7. In Table 7, the injection time for center inlet at 160°C was recorded by counting the time between the resin flowing into the inlet and flowing out of the outlets at the mold corners. The shortest time corresponds to the outlet where resin flows out first; and the outlet where resin flows out last determines the longest time. As shown in Fig. 4, the resin flow-front is an elliptic shape and the resin impinges on the side of the mold first, and then flows to the corners. It reflects the combined effects of the anisotropic

nature of the fabric preform and the edge effect. It is interesting to note that a complete wet-out of the preform was obtained in plates molded with either the center inlet or the perimeter inlet injection strategy. Similar ultrasonic attenuation by the C-scan image was obtained from both plates and the void contents are comparable for both plates based on the results of the image analysis. Abraham *et al.* (4) and Hansen (22) found that the perimeter inlet gives much better control of the mold filling and the part quality as compared with the center inlet in the RTM process. Cai (23) demonstrated the mold filling time is lowered substantially in perimeter inlet compared with center inlet in a simplified RTM process analysis. However, this was not the case in this study. On the other hand, as shown in Fig. 5, the viscosity of PR500 resin is as low as 500 mPa · s for a time period of 50 minutes at 150°C, which is suitable for RTM processing and a complete wet out the fabric preform. Apparently, the marked reduction in flexural strength (Table 5), storage modulus (Table 6) and the longer filling time (Table 7) for the plate injected at 150°C via a perimeter inlet can be attributed to the effect of injection temperature. In industrial processes, temperature variations in the production of large composite

Table 7. Effect of Resin Injection Temperature and Fabric Structure on the Mold Filling Time With Different Flow Arrangement.

Fabric/Resin	Mold Filling Time (sec)	
	Center Inlet (160°C)	Perimeter Inlet (150°C)
EF420/PR500	30–78	81
1581/PR500	67–105	147

* Injection pressure: 392kPa.

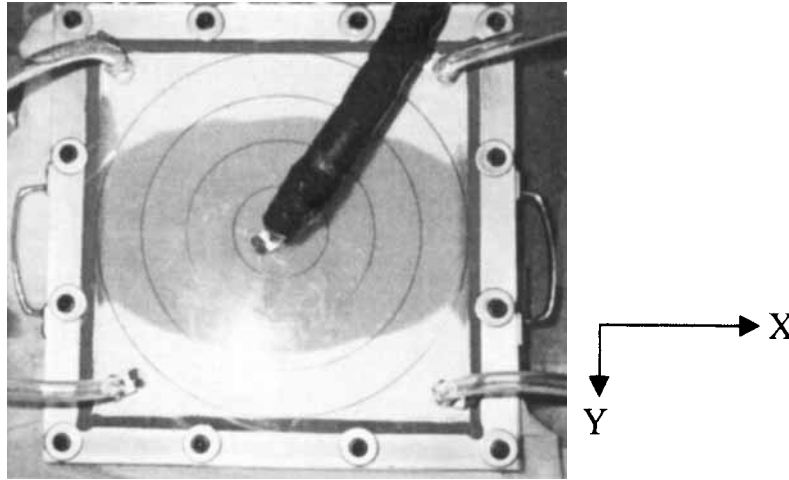


Fig. 4. Photograph of the disruption of resin flow at the edge of a rectangular mold preplaced with EF420 fabrics.

parts with complex geometry could be as large as 11°C (20°F); the quality of the resulting parts is usually inspected by ultrasonic scanning to determine the defects, such as voids, delaminations.

It may be of significance to note the effect of 150°C injection temperature, which is in the margin of hardener's melting temperature (155°C), on the mechanical performance of the parts, although they showed a good quality, based on the results of ultrasonic examination. These marked reductions in flexural strength

and storage modulus for the plate injected at 150°C may be caused by the insufficient mixing of the resin resulting from the particulate filtration of hardener in PR500 by fabric preform resin during the mold filling stage via perimeter inlet. This is because the peak melting temperature of PR500 resin is around 155°C (17), and the melting of the solid hardener is not complete at 150°C. These results, therefore, indicate that resin injection at optimum temperatures is critical in the RTM processing of PR500 resin.

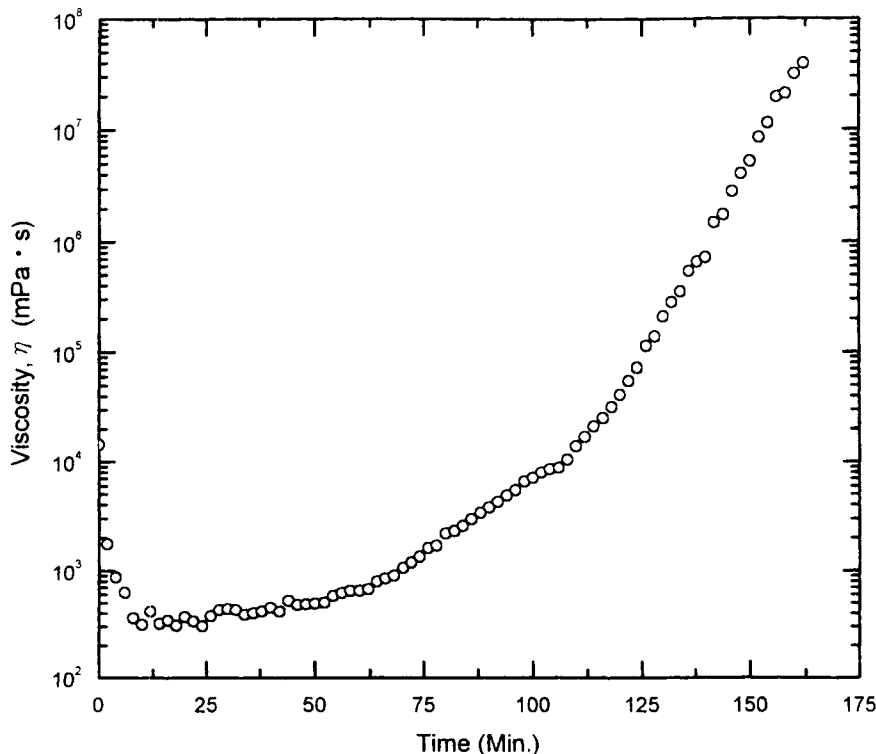
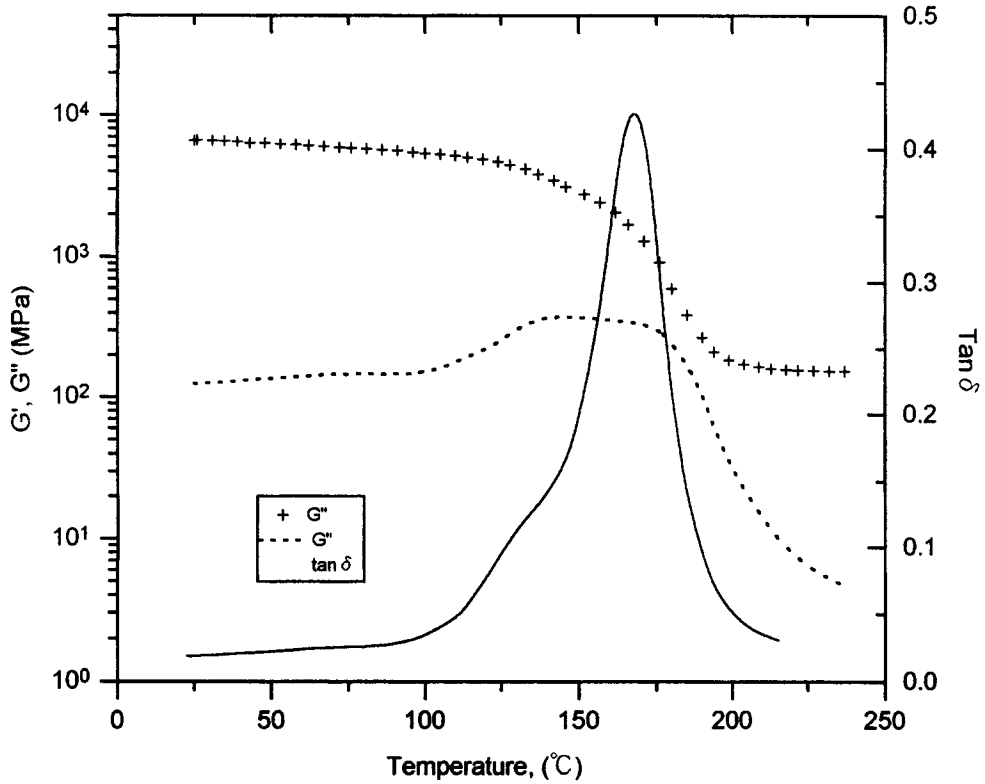
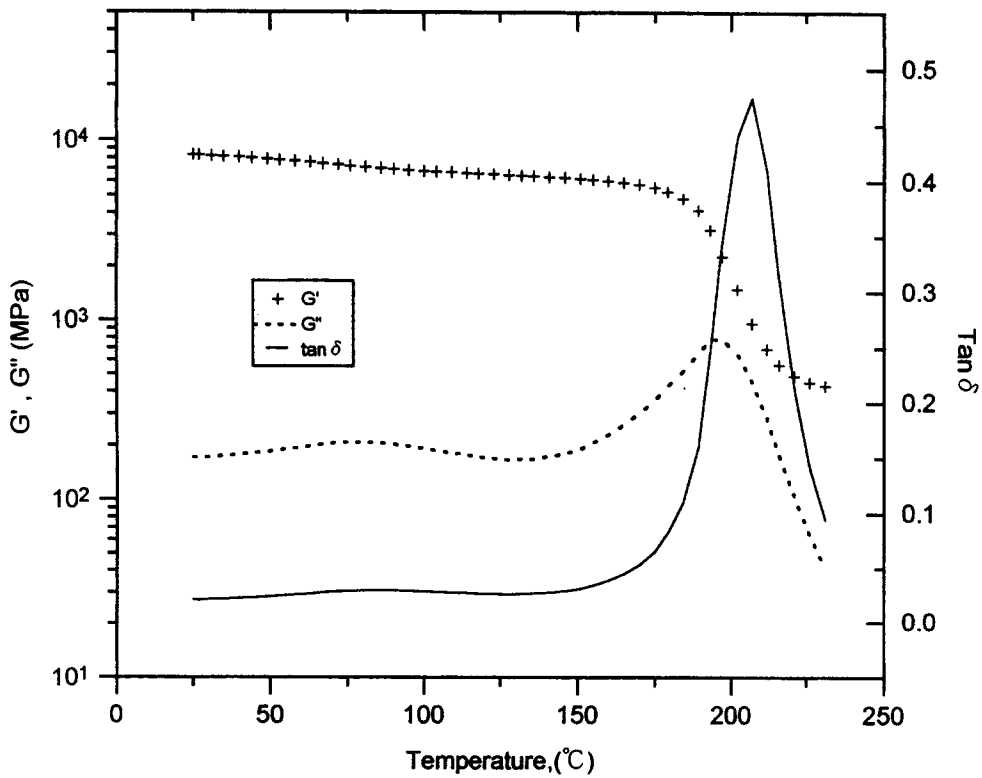


Fig. 5. Viscosity profiles as a function of time at 150°C of PR500 resin.



(a)



(b)

Fig. 6. Effect of different fabrics on the dynamic mechanical properties of fiberglass/PR500 RTM moldings over 25–240°C temperature range; (a) EF420 fabric, (b) 1581 fabric.

Effect of Fabric Structure

The plates containing 1581 eight-harness satin fabric have less void content than the plates containing EF420 fabric in the case of center inlet at 160°C, as given in Table 5. This may be attributed to a more complex flow pattern resulting from EF420 fabric, as shown in Fig. 4. In this flow setup, a square mold with a centrally located gate was used. The resin flow in the highly permeable fabric EF420 was much faster in the x-direction than in the y-direction. As the resin flow front reached the mold edge, a gap developed between the fabric and the mold edge. This gap can create a preferential flow path for the resin, and thus the resin has a tendency of channeling between the fabric preform and the mold edge, which disrupts the filling of the mold cavity. Such flow perturbation is called the edge effect (24). The edge effect could allow large pockets of air to be trapped as the resin reaches the mold corners and meet other flow fronts, possibly causing dry spots, that is, there will be more turbulence and a greater tendency for entrapment of air. Hence, a more complex flow pattern would give a higher void content in the RTM molding (20). The ILSS decreased with increasing void content, as given in Table 5.

The dynamic mechanical behavior of the specimen reinforced with varied fabrics is presented in Fig. 6a and 6b. A distinct difference was found between EF420 and 1581 fabric composites. The storage modulus (G') at the T_g (peak temperature of $\tan \delta$) of EF420 fabric composites showed 32%–60% decreases as compared with those for 1581 fabric composites, as given in Table 6. In Fig. 6a, the peak of loss modulus G'' appeared at a lower temperature accompanying with a plateau, and storage modulus G' decreased significantly at T_g in the EF420 fabric composites. But in 1581 fabric composites, as shown in Fig. 6b, the peak of loss modulus G'' occurred at the much higher temperature and the storage modulus G' retained unchanged until the peak of $\tan \delta$ appeared. As a consequence, there is a large difference in the storage modulus G' at T_g between these two composites. In addition, the flexural modulus of the 1581 fabric plates was 18% higher than that of the EF420 plates, as indicated in Table 5. The possible explanation for this difference could be that the specially designed meso-scale architecture in EF420 led to degradation of the mechanical properties of continuous fiber reinforced composites because of the large resin-rich areas resulting from the uneven fiber distribution (25, 26). However, the significant reduction in mold filling time for the moldings with EF420 fabric, as shown in Table 7, reveals the flow-enhancing characteristics of the mesoscale architecture in EF420 fabric.

CONCLUSIONS

Variation in injection pressure and temperature were found to have a significant effect on the quality and the mechanical performance of RTM fabric composites

based on PR500 epoxy resin system. The optimal resin flow and mechanical performance of 1581/PR500 RTM composite can be attained under 392 kpa injection pressure at 160°C. Moldings of 1581/PR500 by injecting the resin at 150°C resulted in a 41% reduction of storage modulus, a 7% decrease of flexural strength, and a 40% increase in filling time as compared with those injected at 160°C. Fabric structure plays an important role in the flow pattern, filling time and void formation during the mold filling stage. RTM plate reinforced with low permeable 1581 fabric displayed better mechanical properties than the EF420 highly permeable fabric. Molding with EF420 fabric led to a 26% decrease in filling time versus that of 1581 fabric.

ACKNOWLEDGMENTS

The authors wish to acknowledge financial support from the National Science Council, Taiwan, Republic of China, under Grant No. NSC 87-2623-D-009-005. We also wish to thank 3M Co. for providing PR500 resins used in the present work.

REFERENCES

1. D. Stover, *High-Performance Composites*, Jul./Aug. 1994, p. 18.
2. J. Lewis, *Compos. Manufact.*, **5**, 95 (1994).
3. K. F. Karlsson and B. T. Astrom, *Composites Part A*, **28A**, 97 (1997).
4. D. Abraham and R. McIlhagger, *Composites Part A*, **29A**, 533 (1998).
5. J. A. Holmberg and L. A. Berglund, *Composites Part A*, **28A**, 513 (1997).
6. W. B. Young, *J. Compos. Mater.*, **29**, 2192 (1995).
7. C. Hasko, H. B. Dexter, A. Loos, and D. Kranbuehl, *J. Adv. Mater.*, Oct. 1994, p. 9.
8. S. W. Beckwith and C. R. Hyland, *SAMPE J.*, **34**, 7 (1998).
9. V. P. McConnell, *SAMPE J.*, **34**, 37 (1998).
10. R. S. Parnas and F. R. Phelan Jr., *SAMPE Quarterly*, Jan. 1991, p. 53.
11. A. W. Chan and R. J. Morgan, *Polym. Compos.*, **14**, 335 (1993).
12. A. W. Chan and R. J. Morgan, *SAMPE Quarterly*, Apr. 1992, p. 48.
13. T. S. Lundstrom and B. R. Gebart, *Polym. Compos.*, **15**, 25 (1994).
14. N. Patel, V. Rohatgi, and L. J. Lee, *Polym. Compos.*, **14**, 161 (1993).
15. C. D. Rudd, M. J. Owen, and V. Middleton, *Mater. Sci. Technol.*, **6**, 656 (1990).
16. J. S. Hayward and B. Harris, *SAMPE J.*, **26**, 39 (1990).
17. C. L. Lee, J. C. Ho, and K. H. Wei, *Polym. Eng. Sci.*, this issue, Part I.
18. K. Han and L. J. Lee, *J. Comp. Mater.*, **30**, 1458 (1996).
19. S. R. Ghiorse, *SAMPE Quarterly*, Jan. 1993, p. 54.
20. A. W. Chan, D. E. Larive, and R. J. Morgan, *J. Compos. Mater.*, **27**, 996 (1993).
21. W. B. Young, *J. Comp. Mater.*, **30**, 1191 (1996).
22. R. S. Hansen, *Soc. Manufact. Eng. (SME) Tech. Paper*, EM90-214 (1990).
23. Z. Cai, *J. Compos. Mater.*, **26**, 1310 (1992).
24. R. Gauvin and F. Trochu, *Polym. Compos.*, **19**, 233 (1998).
25. P. R. Griffin, S. M. Grove, F. J. Guild, P. Russell, and J. Summerscales, *J. Microscopy*, **177**, 207 (1994).
26. D. M. Basford, P. R. Griffin, S. M. Grove, and J. Summerscales, *Composites*, **26**, 675 (1995).